Hindawi Publishing Corporation
International Journal of Rotating Machinery
Volume 2014, Article ID 625876, 14 pages
http://dx.doi.org/10.1155/2014/625876

Research Article

Improvement of Moderately Loaded Transonic Axial Compressor Performance Using Low Porosity Bend Skewed Casing Treatment

Dilipkumar Bhanudasji Alone,[1] S. Satish Kumar,[1] Shobhavathy M. Thimmaiah,[1] Janaki Rami Reddy Mudipalli,[1] A. M. Pradeep,[2] Srinivasan Ramamurthy,[3] and Venkat S. Iyengar[1]

[1] *Propulsion Division, CSIR-NAL, Bangalore 560037, India*
[2] *Indian Institute of Technology Bombay, Powai 400076, India*
[3] *National Civil Aircraft Development (NCAD), CSIR-NAL, Bangalore 560017, India*

Correspondence should be addressed to Dilipkumar Bhanudasji Alone; dilipbalone@nal.res.in

Received 26 May 2014; Accepted 17 September 2014; Published 23 October 2014

Academic Editor: Jiun-Jih Miau

This paper presents experimental results of a single stage transonic axial flow compressor coupled with low porosity bend skewed casing treatment. The casing treatment has a plenum chamber above the bend slots. The depth of the plenum chamber is varied to understand its impact on the performance of compressor stage. The performance of the compressor stage is evaluated for casing treatment and plenum chamber configurations at two axial locations of 20% and 40%. Experimental results reveal that the stall margin of the compressor stage increases with increase in the plenum chamber volume. Hot-wire measurements show significant reduction in the turbulence intensity with increase in the plenum chamber volume compared to that with the solid casing at the stall condition. At higher operating speeds of 80% and at 20% axial coverage, the stall margin of the compressor increases by 20% with half and full plenum depth. The improvement in the peak stage efficiency observed is 4.6% with half plenum configuration and 3.34% with the full plenum configuration. The maximum improvement in the stall margin of 29.16% is obtained at 50% operating speed with full plenum configurations at 40% axial coverage.

1. Introduction

Instabilities in the compression systems of aero engines are the greatest issues of concern for all the gas turbine community. The new generations of aero engines demand fewer compressor stages to cut down the weight; at the same time it demands relatively higher distortion tolerance. This unique requirement gives rise to another challenge for the designers of the compression system to develop the compressors with higher loading per stage. This requirement further narrows down the safer operating range of the compressors and makes the compressors stages more prone to the instabilities like surge and stall in the absence of any control devices. Given the potential catastrophic consequences of compressor stall, there is considerable incentive for developing methodologies that can extend the stable operating range of compressors/fans. Many active and passive methods of improving the operating range of compressors/fans are in existence. The active methods like air jets and oscillating inlet guide vanes are not still used in aircraft engines. Passive methods like blade sweep, casing treatments and reshaped casings, blowing, and injections are the most popular methods and thus are preferred to improve the operating range of the compressors/fans. Casing treatment is one of the techniques which are immensely popular in delaying the onset of these instabilities and in extending the operating range of the compression system to lower mass flow rates. However, casing treatments can be applicable only to rotors which are prone

to instabilities in tip regions or so-called tip critical rotors [1]. These benefits can thus pass on the aero engines which can sustain greater inlet distortion tolerance. Casing treatment or placing a porous casing around the rotor tip is in effect a technique to control the casing boundary layers and thus delay the occurrence of the instabilities. This fact has been confirmed by several investigators [1–20].

Pioneering work was done by Koch [2] of General Electric, USA, who experimentally studied the effect of outer casing blowing or bleeding in a typical transonic compressor stage with and without inlet flow distortion. Both blowing and bleeding produce significant improvement when stall initiates at the tip. In the case of stall initiation away from the tip, the casing bleed had an adverse effect on the stall limit. It was also observed that the mere presence of a porous casing around the rotor tip was sufficient to cause a marked improvement in the stable flow range. This led to the development of casing treatment and a series of investigations were initiated by NASA [3–5] to evaluate the effect of various treatment geometries on stall margin and overall performance of axial compressors. Parametric studies on axially and radially skewed slots as well as on circumferential grooves were carried out by Guruprasad [6] in a transonic compressor stage. While the axial/radial skewed slots improved stall margin by almost 25%, the circumferential grooves produced only marginal improvement. Experiments were carried out for different tip clearances, porosity levels, and axial coverage of the treatment slots as well as for different rotor tip speeds. The detailed studies revealed an optimum axial coverage of the treatment slots over the rotor tip. It was also concluded that higher stall margin gains with minimum efficiency penalty can be achieved by optimizing various parameters of casing treatments.

Takata and Tsukuda [7] carried out experiments on a low speed, single stage compressor with axial as well as skewed slot casing inserts and with varying rotor tip clearances. They were the first to report clear evidence of the importance of orientation of skewed grooves on the improvement of stall range and performance. The maximum improvement in the stall margin was noticed when the slots were skewed opposite to the rotor rotation. Fujita and Takata [8] have shown a very close correlation between the increase in stall margin and the loss in efficiency.

Smith and Cumptsy [9], on a low speed isolated rotor with axial skewed slot casing treatment, showed that the removal of high swirl, high loss fluid from the trailing end and its reintroduction into the main flow near the leading end is mainly responsible for the effectiveness of the casing treatment.

Adams and Smith [10] studied six axial casing treatment configurations with porosity of 69% with radial skewed angle varying from +60° to −60°. The maximum improvement in stall margin of 20% above the solid casing was noticed with +45° skewed. It was concluded from the above studies that an angle of skew of +45° would be most beneficial. Emmrich et al. [15–17] carried out numerical and experimental analysis of a single stage subsonic compressor coupled with skewed casing treatment with a porosity of 67%. The slots were inclined to the axial direction by 15° and to the radial by 45° in the direction of rotation. The performance of the compressor in the presence of skewed casing treatment was evaluated for different axial coverage of rotor chord varying from 38% to 46%. The experimental and numerical analysis showed the 38% coverage as the best configurations.

Zhu et al. [11–14] experimentally and numerically evaluated the influence of an axial and bend skewed groove casing treatment on the performance of an isolated rotor with a pressure ratio of 1.249 and mass flow rate of 5.6 kg/s. The porosity was 67% and the numbers of slots were 184. Results showed considerable improvement in the stall margin without efficiency penalty. In this recent development, it was shown to be possible to improve the efficiency of the transonic axial flow compressor stage with axial slots casing treatment with the rotor redesign [19]. Voges et al. [20] carried out interesting measurements with bend skewed casing treatments on transonic stage at 20% axial coverage and observed that there is exchange of fluid between rotor passage and casing treatment slots due to pressure differential. It was observed that, at the stall condition, the periodical injection of energized fluid out of the casing slots stabilizes the tip clearance vortex and thus delays the onset of stall.

The majority of the literatures dealt with casing treatment geometries with higher porosities and reflect losses in the stage efficiency. The bend skewed casing treatment has a potential of improving the stall margin without sacrificing the efficiency. However, very limited published literature reports this type of casing treatment. This was the motivation for studying the performance of a transonic axial stage in the presence of lower porosity bend skewed casing treatment at two axial configurations (20% and 40%). In addition to this, an attempt has also been made to understand the unexplored parameter of the plenum chamber volume coupled to this casing treatment. The performance of the compressor stage in terms of stall margin improvement, efficiency, and nature of stall was studied experimentally for different plenum chamber volume. The experimental results are compared with the compressor stage performance in the presence of the solid casing. The variation of the inlet axial velocity in the tip region at stall condition is also studied using a single component hot wire probe for the solid casing and casing treatment.

2. Descriptions of the Research Facility

Experimental investigations were carried out in the open circuit axial flow compressor research facility of the Propulsion Division of CSIR-National Aerospace Laboratories, Bangalore. The schematic of the test facility with different measurement planes is shown in Figure 1. The compressor stage is driven by a variable speed DC motor with a power rating of 1.15 MW at 1000 rpm, through a speed increasing gearbox of 1 : 18 gear ratio and an electronic torquemeter. The speed of the motor was controlled precisely within ±1 rpm using a speed controller and a feedback system. Air enters through the inlet bellmouth, gets compressed in the research compressor stage, and discharged to the atmosphere after passing through an axi-radial diffuser, volute casing, venturimeter, and the exit throttle valve. Mass swallowed by

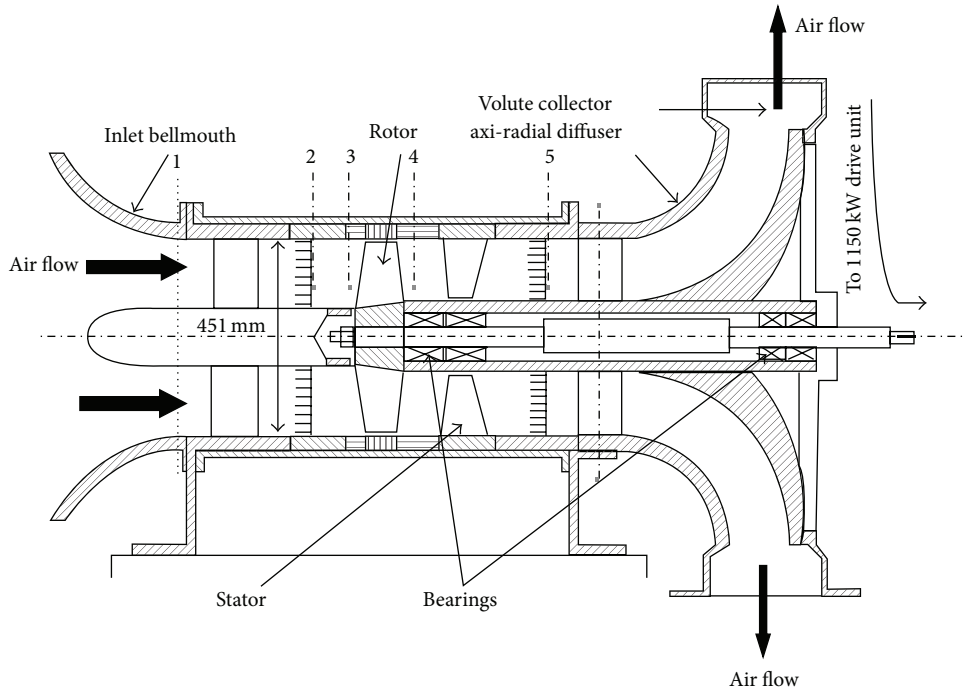

Figure 1: Schematic of the single stage transonic axial flow research compressor.

the compressor is measured by the calibrated inlet bellmouth as well as the exit venturimeter. The mass flow rate is then corrected using sea level and local ambient conditions. The power input to the compressor stage is measured using the electronic torquemeter. Four total pressure rakes each comprising 15 radially stacked pitot tubes located at the stator exit at measurement plane 5 and inlet total pressure measured at plane 2 are used to derive the stage total pressure ratio developed by the compressor. Two precalibrated K-type thermocouples one at the rotor inlet and the other at the stator exit are used to measure the air flow temperature. The mass flow rate through the compressor stage is precisely controlled using butterfly-type exit throttle valve. This valve has provision to close gradually to locate the exact stall inception point. All the pressures and temperatures are acquired using National Instrument's LabVIEW based high speed data acquisition system. Electronic pressure scanners are used for acquiring the pressures from the research compressor test bed. An aerodynamic probe is traversed at the rotor exit to measure the various flow parameters like flow angle and Mach numbers. A single component hot wire probe along with Constant Temperature Anemometer (CTA) is used for acquiring the time dependent unsteady velocity signals. The variation in the axial velocity is measured using the hot wire probe located in the tip region and ahead of the rotor leading edge. To cater the entire velocity range the probe was calibrated till 190 m/s velocity. The real time signals were acquired at full flow and near stall condition for the solid casing and casing treatment configurations. The detailed specifications of the moderately loaded compressor stage are given in Table 1. Different combinations of spacer's rings are employed to get the desired axial coverage of the casing

Table 1: Design specifications of the transonic compressor stage.

Stage	Single transonic
Stage total pressure ratio	1.35 : 1
Corrected mass flow rate	22 kg/s
Number of rotor blades	21 (transonic)
Number of stator blades	18 (subsonic)
Corrected rotational speed	12930 rpm
Relative Mach number	1.15 (tip)

treatment. The two axial coverages of 20% and 40% relative to rotor leading edge are identified for the present experimental study. The cold tip clearance is measured before the assembly for the solid casing and all configurations of casing treatments. It is kept at 1% of the rotor blade tip chord. All the measurements are observed to be within ±1% accuracy.

3. Casing Treatment Configurations

The casing treatment designed for the present experimental study is the bend skewed type with porosity of 21%. The porosity gives the percentage open area and was based on the width of the slots and supporting rib width. The axial length of the casing treatment slots is kept equal to the axial blade chord at the rotor tip section. The treatment has 63 slots with depth of the slots is 11 mm. The slots inlet segment is axial and rear segment is skewed by 45° following the rotor blade stagger. The axial length of both the segments was kept half of the rotor chord. Both the segments are inclined at 45° in the radial plane in such a way that the flow is emerging from the casing slots in the counterclockwise direction. The width of

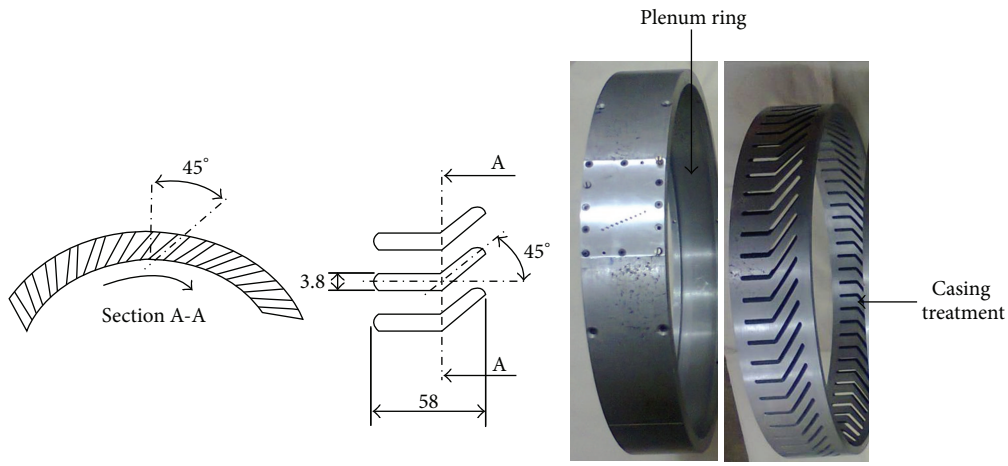

Figure 2: Schematic and photograph of the casing treatment and plenum chamber ring.

the treatment slots is 3.8 mm and is equal to the maximum thickness of the rotor blade. Figure 2 shows the fabricated casing treatment and plenum chamber ring used for the experimental evaluations. The plenum chamber is placed above the casing slots and has maximum depth of 11 mm. This depth is varied in two stages to get the different plenum chamber volume. In the first step, the plenum chamber with zero depth is tested and this configuration of the casing treatment is designated as CT3-NP. In another configuration, the plenum chamber depth is equal to half of the slot's depth and this combination is designated as CT3-HP. In the last and final configuration, the depth of plenum chamber is equal to the depth of the slots and hereafter will be referred to as CT3-FP. All these configurations are tested at axial coverage of 20% and axial coverage of 40% relative to the rotor leading edge. Figure 3 shows the casing treatment with three configurations of plenum chamber placed above the rotor at 20% axial coverage relative to the rotor leading edge.

4. Results and Discussions

The compressor stage operating envelop is obtained for the solid casing and various casing treatment configurations. The overall envelop with casing treatment is compared with the solid casing. The stall margin improvement (SMI) above the solid casing is evaluated at different operating speeds and for all the configurations of the casing treatment. The operating envelop is generated by operating the compressor at constant speeds and measuring the mass flow rate, stage total pressure ratio, and the efficiency. The variation of the stage total pressure ratio and the efficiency versus corrected mass flow rate gives the operating envelop of the compressor stage.

4.1. Compressor Performance Envelop. The performance envelop of the compressor stage is developed by operating the stage at different speeds and closing the exit throttle valve till the instability in the flow initiates. At each constant speed line, the mass flow rate, stage pressure ratio, and stage efficiency are measured. The mass flow rate is then corrected using sea level and the local operating conditions. The steady state measurements are not carried out for the solid casing within stall due to abrupt stalling characteristics and chances of compressor damage. The measurements are restricted till the prestall points. The comparative performance envelop for the solid and casing treatments configurations are plotted at two different axial locations of 20% and 40%. An improvement in the stall margin and variation of the stage efficiency are studied.

4.1.1. Compressor Performance Envelop at 20% Axial Coverage (0.2C). Figure 4 shows the comparative variation of the stage total pressure ratio and adiabatic efficiency of the compressor stage for the solid casing and casing treatment with different plenum configurations at 20% axial coverage. Figure 5 gives the percentage improvement in the stall margin above the solid casing with all the configurations of the casing treatment at different operating speeds. The loss and/or gain in the peak stage efficiency above the solid casing is given in the Figure 6. For the solid casing, the stage total pressure ratio and mass flow rate delivered by the compressor stage increases with the operating speed. Each operating line shows gradual increase in the pressure ratio till the peak value. The decrease in the mass flow rate is gradual with the closure of the exit throttle valve. After the peak pressure, with smaller closure of exit valve, there is a sudden drop in the stage pressure ratio, mass flow rate, and efficiency. The compressor stage, therefore, exhibits an abrupt nature of stall inception. The steady state measurements are restricted in this region as the stage operation leads to excessive vibrations. All the measurements are restricted till 80% of the design speed. The peak stage efficiency decreases with increase in the operating speeds. A drop of about 3.8% in the peak stage efficiency is noticed from 50% operating speed to 80% speed. A peak stage efficiency of 86% is recorded at 50% design speed. The peak stage pressure ratio of 1.242 is observed at a prestall mass flow rate of 16.63 kg/s and at 80% of the design speed. At full flow conditions at this speed, the compressor delivers 19.44 kg/s and has short stable operating range before going into the abrupt stall beyond 16.63 kg/s. The fast degradation in

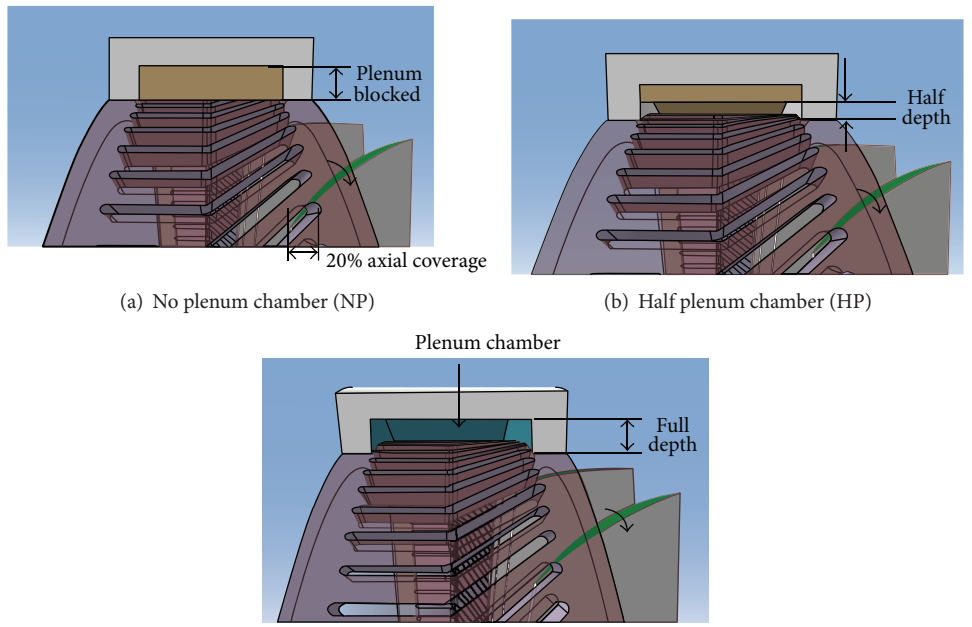

(a) No plenum chamber (NP)

(b) Half plenum chamber (HP)

(c) Full plenum chamber (FP)

Figure 3: Casing treatments with three plenum chamber configurations at 20% coverage.

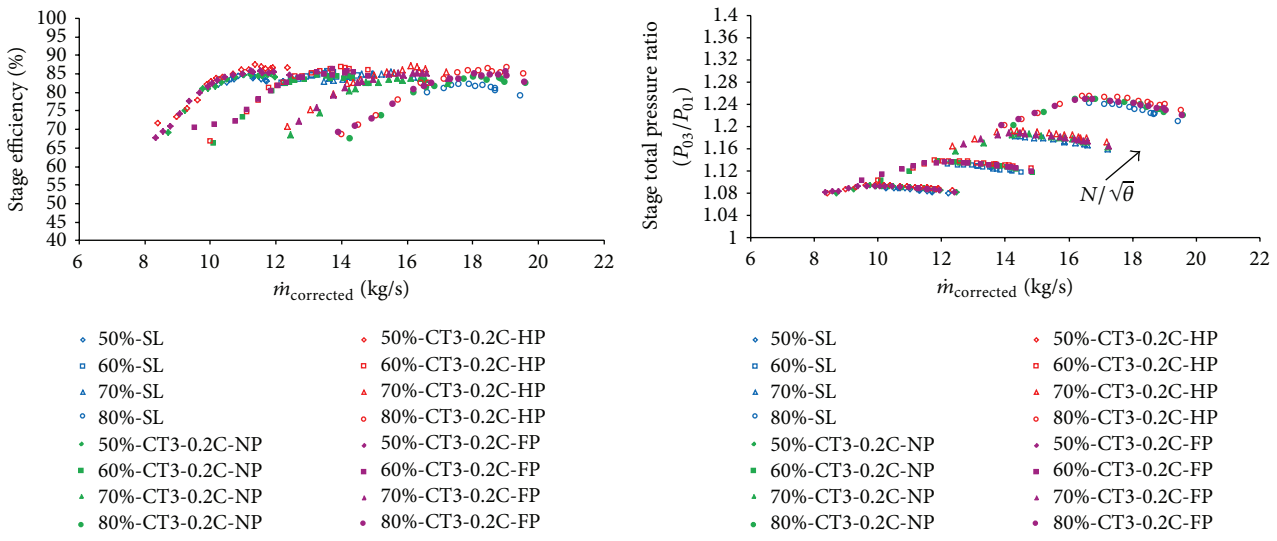

(a) Variation of stage efficiency with mass flow rate

(b) Variation of stage total pressure ratio with mass flow rate

Figure 4: Compressor operating envelop with solid casing and casing treatment at 20% axial coverage.

the stage efficiency shows the severity of the losses incurred due to various viscous effects in the tip region at higher operating speeds.

At 20% axial converge with CT3-NP casing treatment configuration, the degradation in the stage efficiency is not severe with operating speeds as compared to the solid casing. The peak stage efficiency degraded by about 1.1% compared to 3.8% with solid casing at 80% operating speed. The stage efficiency was lower than the solid casing till 70% design speed. At 80% design speed, the casing treatment shows improvement of about 2% over the solid casing in the peak stage efficiency. This is because of the ability of the casing treatment to minimize the detrimental effects associated with the tip leakage flow. At all the operating speeds, casing treatment maintains marginally higher pressure ratio as compared to the solid casing. One of the reasons for lower efficiency till 70% speed is more power input required for the compressor to maintain the marginally higher pressure ratio.

At all the operating speeds, the compressor stalls at much lower mass flow rates and results in improvement in the stable

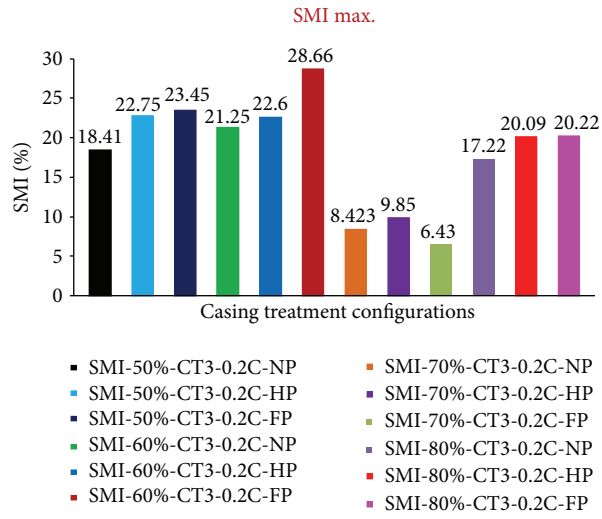

FIGURE 5: Stall margin improvements with casing treatment-plenum chamber configurations at 20% axial coverage.

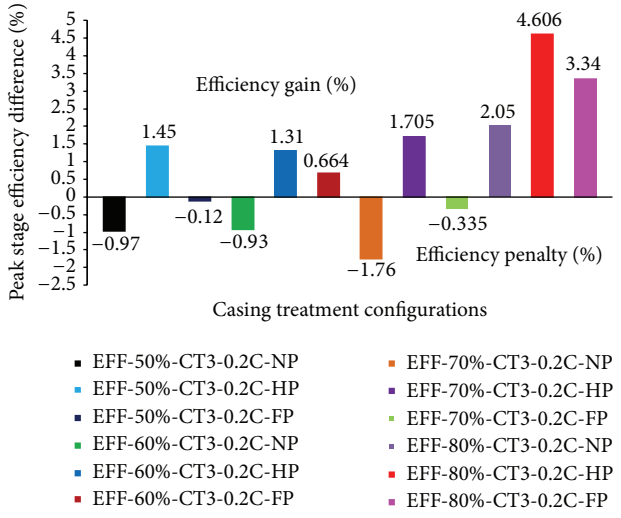

FIGURE 6: Gain and loss in peak stage efficiency with casing treatment-plenum chamber configurations at 20% axial coverage.

operating range. The peak stage pressure ratio occurred at lower mass flow rate as compared to that of solid casing because it is possible to operate the compressor at relatively higher incidence with casing treatment. After the peak, the pressure ratio drops gradually, but the compressor stage maintains stable operations. The maximum improvement in the stall margin obtained is 21.25% at 60% operating speed. This configuration gives optimum performance at 80% design speed with 17.22% improvements in the stall margin and with 2.05% gain in the stage efficiency.

CT3-HP configuration shows significant improvement in the stage performance in terms of stall margin and efficiency gain. In this configuration, the plenum chamber depth is equal to half the slot depth. Additional volume of the plenum chamber allows fluid to get settled and injected back into the primary flow. The tip leakage flow enters the plenum chamber through the casing slots and thus weakens the tip leakage flow. This phenomenon improves the compressor pressure recovery and also the stage efficiency. All the operating speeds show improvement in the stage efficiency above the solid casing. At 80% design speed, the improvement in the peak stage efficiency was 4.6% with 20% improvement in the stall margin. For this configuration at this coverage, CT3-HP gives the best performance.

For the CT3-FP configuration with additional increase in the plenum volume, the compressor performance in terms of stall margin improvement increases further at all the operating speeds except at 70%. This configuration also shows effectiveness at 80% design speed with 20.22% improvement in the stall margin and 3.3% gain in the peak stage efficiency. At 50% and 70% design speed, the peak stage efficiency decreases marginally by 0.2% as compared to solid casing with recovery in the stage pressure ratio.

For this axial coverage, the maximum improvement in the stall margin obtained is 28.66% at 60% operating speed for CT3-FP configurations and can be seen from Figure 5. From Figure 6 it is clear that, at this axial coverage, all the CT3-HP combinations give an improvement in the peak stage efficiency for all the operating speeds. At higher operating speed of 80% all the configurations of casing treatments improve the stage efficiency.

4.1.2. Compressor Performance Envelop at 40% Axial Coverage (0.4C). At 40% axial coverage, 40% of the casing treatment slots are exposed to the rotor blade tip. With CT3-NP configuration, the improvement in the stall margin is slightly lower than 20% axial coverage at all the operating speeds. The peak stage pressure ratio shows marginal reduction than the previous coverage but maintains relatively higher than that with the solid casing. This configuration results in significant drop in the peak stage efficiency as compared to the solid casing and 20% axial coverage. This reduction in the peak stage pressure ratio and efficiency is due to interaction of the tip flow with casing slots. Rotor requires more work to overcome the slot resistance and maintain the stage pressure ratio and mass flow rate. This results in higher torque input and therefore leads to drop in the efficiency. Figure 7 shows the comparative variation of the stage total pressure ratio and the adiabatic efficiency of the compressor stage with solid casing and casing treatment with different plenum configurations at 40% axial coverage. Figures 8 and 9 summarize the compressor stage performance in terms of stall margin improvement and efficiency variations. Figure 8 shows the improvement in the stall margin above the solid casing with all configurations of casing treatment at different operating speeds. From Figure 8 it is clear that maximum improvement in the stall margin of 29.165% is obtained with CT3-FP at 50% speed. Loss and gain in the peak stage efficiency are given in Figure 9. Maximum gain of 2.973% in the peak stage efficiency is obtained with CT3-HP configuration at 80% design speed.

For the CT3-HP case too, the stage performance improves with the increase in the plenum chamber volume. The stage pressure ratio further increases and shows gain in the stage

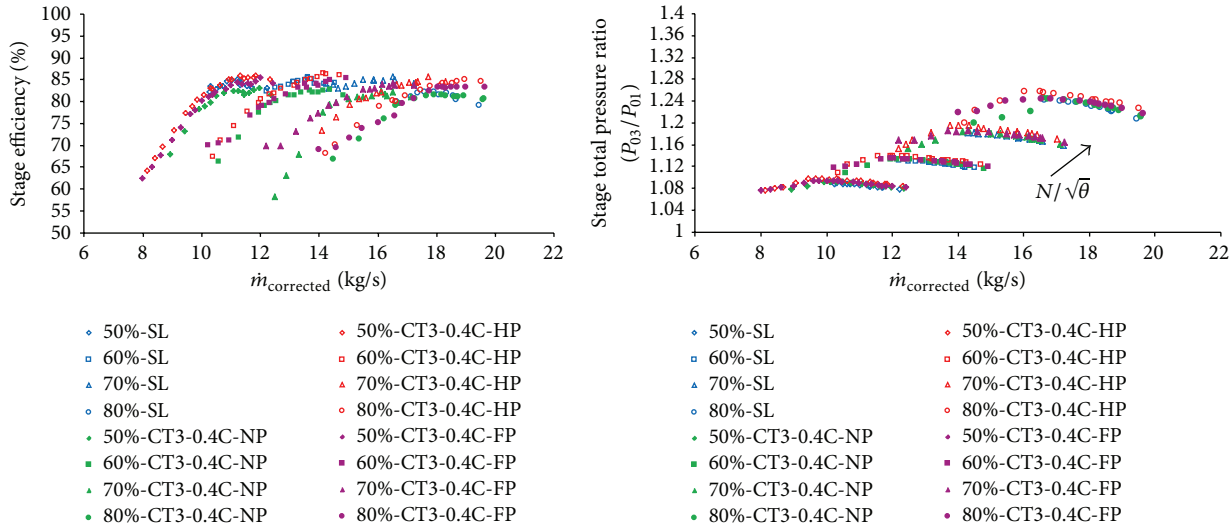

(a) Variation of stage efficiency with mass flow rate

(b) Variation of stage total pressure ratio with mass flow rate

FIGURE 7: Compressor operating envelop with solid casing and casing treatment at 40% axial coverage.

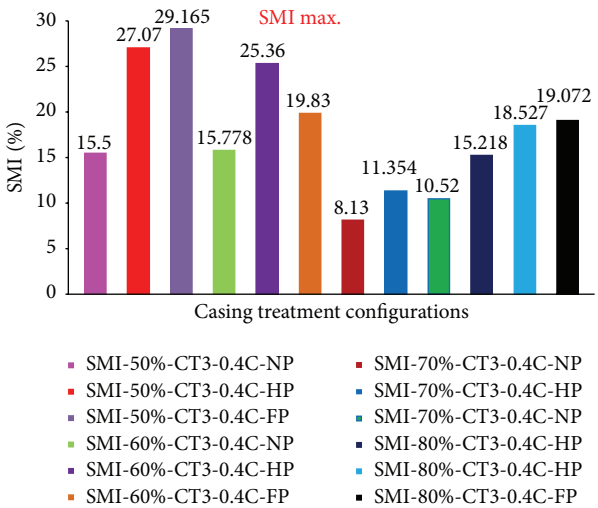

FIGURE 8: Stall margin improvements with casing treatment configurations at 40% axial coverage.

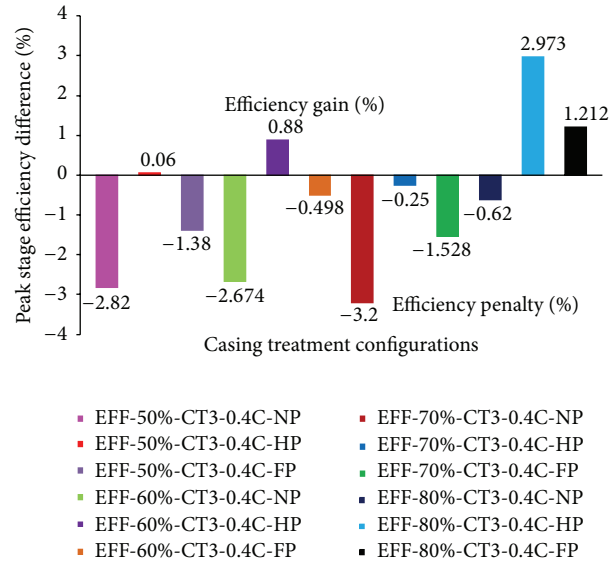

FIGURE 9: Variation of the peak stage efficiency with casing treatment configurations at 40% axial coverage.

efficiency. At all the operating speeds, the stall margin is higher than the CT3-NP configurations. A maximum improvement in the stall margin noticed is 27.07% and 25.36% at 50% and 60% design speed, respectively. This configuration also shows improvement of 2.97% in the peak stage efficiency above the solid casing at 80% operating speed. With further increase in the plenum volume with CT3-FP configurations, the stall margin further increases to 29.16% and 19.07% at 50% and 80% design speed, respectively. However, this increase in the plenum chamber volume causes reduction in the peak stage efficiency at all the operating speeds other than 80% speed as compared to solid casing. At higher operating speed of 80%, all the casing treatment configurations except CT3-NP at 40% coverage show improvement in the stall margin and the peak stage efficiency compared to the solid casing. This shows the positive impact of the casing slots and the plenum chamber in controlling the tip leakage flow and associated detrimental effects.

At both the axial coverages, a CT3-HP configuration gives the best performance and thus shows that there is a distinct relationship between the casing treatment porosity, slot, and the plenum chamber depth.

4.2. Variation of Rotor Exit Flow Parameters. A precalibrated 3-hole aerodynamic probe is traversed at the rotor exit to get the radial variations in the flow parameters. The flow

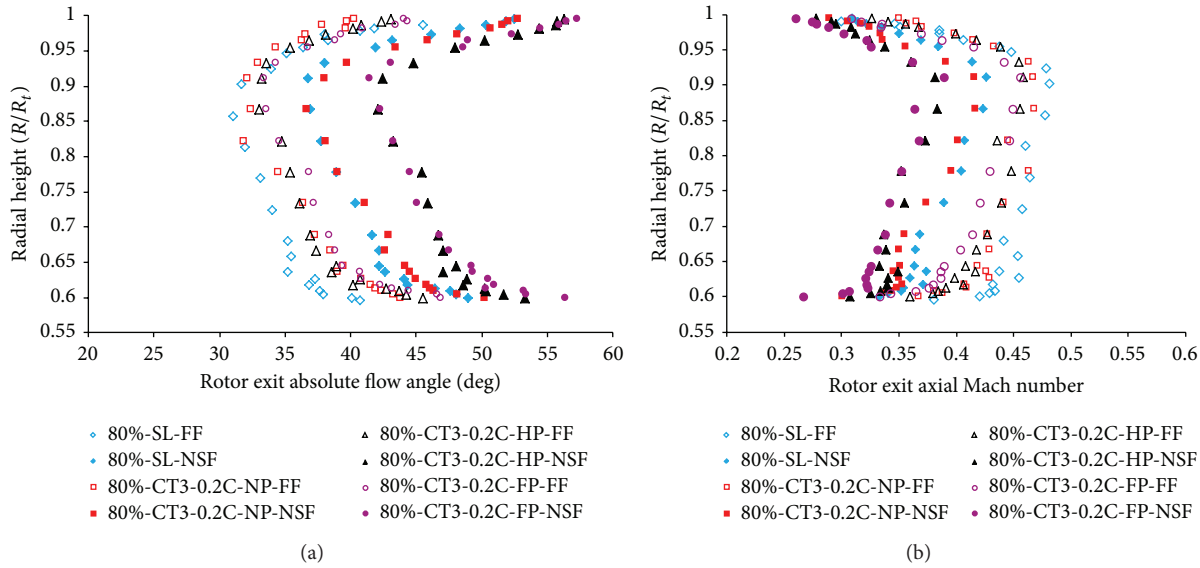

FIGURE 10: Comparative variations of (a) rotor exit absolute flow angle and (b) axial Mach number for the solid casing and three configurations of casing treatment and plenum chamber at full flow (FF) and near stall flow (NSF) conditions.

parameters are evaluated at full flow (FF) and near stall flow (NSF) conditions for the solid casing and casing treatment configurations. Figures 10 to 12 show the comparative variations of these flow parameters at 80% design speeds and at 20% axial coverage. The axial positions of 20% are chosen because, at this coverage, the compressor performance is optimum. The probe is traversed using an automatic probe traverse mechanism with 1 mm resolution within the tip and the hub boundary layers.

4.2.1. Absolute Flow Angle. The rotor exit absolute flow angle gives the angle between the absolute velocity and axial velocity vectors. It is an indicator of the flow swirl and reduction in the axial velocity of the flow at constant tangential speed. Figure 10(a) gives comparative variations of absolute flow angle at the rotor exit with casing treatment and solid casing.

For the solid casing, the flow angle decreases gradually towards the tip region. The hub region shows higher flow angle because of the larger swirl induced by the rotor blade due to higher blade curvature and hub boundary layer. The effect of hub boundary layer is not that significant as the rotor scraps the development of boundary layers. The flow angle decreases gradually till 85% of the blade span and then increases towards the rotor tip regions. This effect seems to be dominating in the 15% blade height from the tip region. Increase in the flow angle is observed to be very sharp in this zone. This increase in the flow angle is due to the reduction in the axial velocity and increase in the boundary layer and tip leakage flow in the tip regions. The maximum flow angle measured is 46° at 99% blade height and minimum of 31° at 85% of blade height. This shows that the tip effects are very dominating in this 14% height. At near stall flow conditions for the solid casing, the flow angle follows similar trends but maintains higher values throughout the blade height. The maximum flow angle recorded is 52° at a blade height of 99%. This increase in the flow angle is due to the reduction in the axial velocity and increase in the back pressure because of the closure of the exit throttle valve.

The CT3-NP, CT3-HP, and CT3-FP configurations do not affect the behavior of the absolute flow angle at the full flow condition. At the near stall flow condition, with CT3-NP, the flow angle is the lowest as compared to the other two configurations. With this configuration, the trends in the flow angle are similar to those observed for the solid casing at both the operating conditions. The CT3-HP and CT3-FP configurations at stall condition record higher flow angle throughout the blade span. In the tip region with these two configurations, increase in the flow angle is very steep because of higher retardation in the axial velocity as can be observed from Figure 10(b). The flow angle increases from 41.41° to 57.4° from 92% to 99% blade height with CT3-FP.

4.2.2. Axial Mach Number. Figure 10(b) shows the comparative variations of rotor exit axial Mach number. At full flow condition, the axial Mach number gradually increases from the hub towards the tip region till 92% of the blade height for the solid and the casing treatment cases. Above 90% blade height, the Mach number decreases because of reduction in the axial velocity. This reduction in the axial Mach number further increases the absolute flow angle and can be observed from the absolute flow angle profile. The axial flow exhibits higher skewness in the tip region due to the various viscous effects associated with the tip leakage flow and the tip boundary layer. At the full flow condition, increase in the plenum volume to FP reduces the suction capability of the compressor marginally and compressor ingests slightly lower mass flow rate. This further reduces the axial velocity and thus results in a lower Mach number as compared to the other two configurations of casing treatment and solid casing. CT3-NP

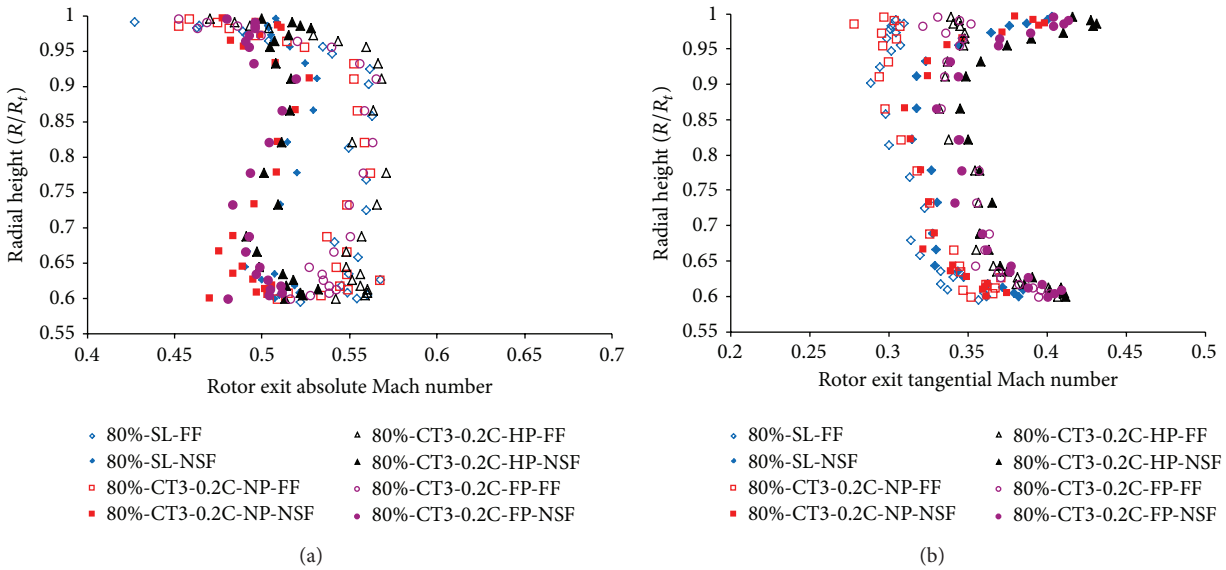

FIGURE 11: Comparative variations of (a) rotor exit absolute and (b) tangential Mach number for the solid casing and three configurations of casing treatment and plenum chamber at full flow (FF) and near stall flow (NSF) conditions.

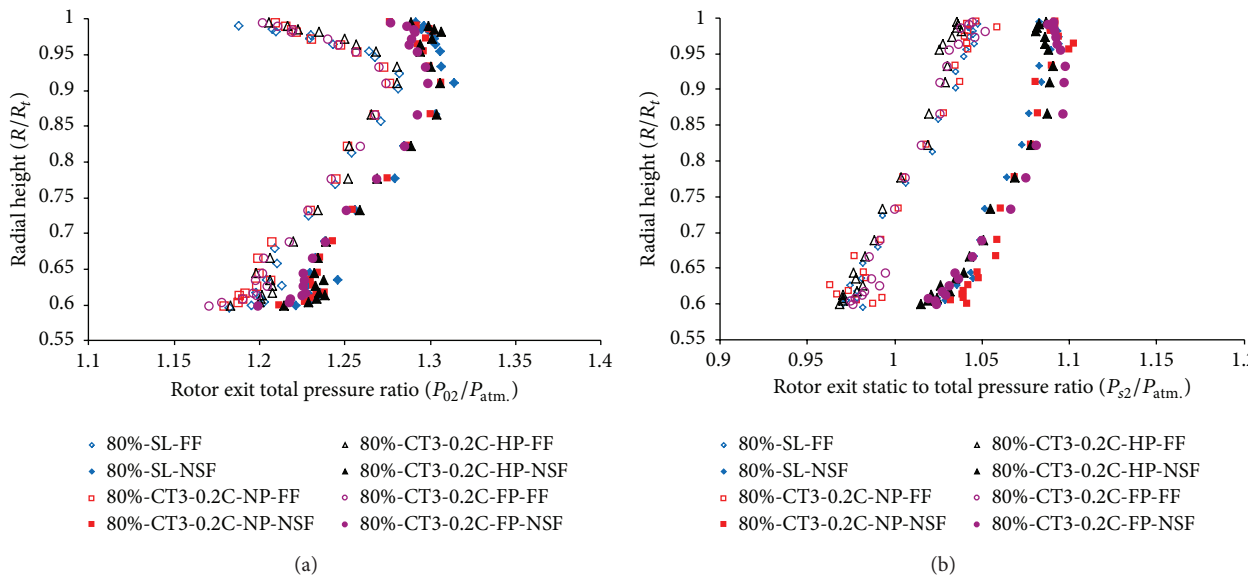

FIGURE 12: Comparative variations of (a) rotor exit total and (b) static pressure for the solid casing and three configurations of casing treatment and plenum chamber at full flow (FF) and near stall flow (NSF) conditions.

configuration and solid casing show the identical distribution of Mach number at full flow condition. This shows that the lower porosity casing treatment does not significantly alter the flow pattern at the full flow conditions. The performance of the compressor with CT3-HP falls in between those observed with CT3-NP and CT3-FP. At near stall conditions, CT3-FP exhibits the lowest axial Mach number throughout the blade height. The lowest Mach number recorded is 0.26 at the rotor tip with CT3-FP. From the above trends, it is clear that lower porosity casing treatment with higher plenum volume can produce relatively higher stall margin.

4.2.3. Absolute Mach Number. The radial variations of absolute Mach number are shown in Figure 11(a). At full flow condition, the absolute Mach number is higher than the axial Mach number. An absolute Mach number of 0.55 is obtained with all the configurations at the full flow condition. The profile is fairly constant in the core region and skewed in the tip region. The lower axial velocity in the tip regions leads to lower values of absolute Mach number in these regions. At near stall flow condition, it further reduces due to increase in the back pressure created by the closure of the exit throttle valve. For the solid casing at near stall flow condition,

the absolute Mach number is higher than that of the full flow condition because of higher tangential velocity component and can be observed from Figure 11(b). CT3-FP configuration results in lower Mach number in the core region as compared to the other configurations. This is because, with the FP configuration, it is possible to throttle the compressor to further lower mass flow rate. In the tip region with all the casing treatment plenum chamber configurations at near stall flow condition, the absolute Mach number is higher than the full flow condition at corresponding blade span.

4.2.4. Tangential Mach Number. Tangential Mach number represents the swirl in the flow. At full flow condition, the swirl gradually decreases towards the tip region for the solid casing and CT3-NP configurations. CT3-HP and CT3-FP configurations show similar trends at the full flow condition but maintain slightly higher values as compared to CT3-NP and solid casing. At near stall flow condition, the tangential Mach number increases in the tip region for all the casing configurations. The lowest tangential Mach number recorded is 0.43 with CT3-HP at near stall flow condition and close to the casing wall. The comparative variation of the tangential Mach number is shown in Figure 11(b).

4.2.5. Total and Static Pressure. Figures 12(a) and 12(b) show the radial variation of total and static pressure along the blade height, respectively. Both the profiles show the characteristics of a tip strong rotor. The total pressure and static pressure increase along the blade height and increase with the exit throttle valve closure. At the full flow operating condition, the total pressure profiles show exact match with the solid casing and all the configurations of casing treatments. The total pressure profile is more skewed in the tip region. The solid casing shows the lowest pressure at the rotor tip as compared to the other configurations because of higher losses incurred by the leakage flow and the boundary layer effects. These losses are controlled by the casing treatments and reflect on the total pressure profiles. The peak total pressure ratio of 1.28 is recorded with CT3-HP configuration. At near stall flow condition, the total pressure ratio increases because of the reduction in the axial velocity. At this condition, the profile skewness decreases in the tip region. The overall pressure ratio developed by the rotor decreases marginally with the increase in the plenum chamber height. The reduction in the pressure ratio, however, is not so severe. At near stall condition, the CT3-FP shows the static pressure recovery because with this casing treatment configuration, the compressor stalls at lower mass flow rate and thus results in higher stall margin improvement.

4.3. Variation of Rotor Inlet Axial Velocity. As the compressor operation shifts from stable operating condition to unstable condition, the inlet axial velocity fluctuates. The fluctuations in the axial velocity are normally more dominant in the tip region. A single component hot wire probe was placed in the tip region to measure the axial velocity fluctuations. The probe was located one rotor chord ahead of the rotor leading edge and 5 mm away from the casing wall. The stall initiates while the compressor operates at constant speed and the exit throttle valve is closed gradually. The hot wire probe was calibrated using the hot wire calibrator setup. The sampling frequency is varied from 20 kHz to 50 kHz for different configurations and for different operating conditions. All the data is acquired and processed offline. FFT is performed to get the dominating frequency for the solid and casing treatment configurations. The hot wire measurements are restricted at 6625 rpm and 7950 rpm, which correspond to 50% and 60% design speed, respectively. All the signals are compared with solid casing at 7950 rpm (60% operating speed).

Figure 13(a) shows the variation in the inlet axial velocity for the solid casing at stall for 0.1 s. At each operating condition, the turbulence intensity is calculated and compared. At this operating speed, with the solid casing, the compressor stage stalls at very high mean velocity of 91 m/s and results in high turbulence intensity of 41%. This can be seen from Figures 13 and 17. Higher mean axial velocity at stall gives relatively higher stalling mass flow rate with solid casing. The variation in the axial velocity was very abrupt from 185 m/s to 8 m/s. This variation in the axial velocity shows the abrupt nature of the rotating stall in the presence of solid casing. Figure 13(b) shows that a single stall cell travels at 70 Hz frequency with very high amplitude of oscillations and with subsequent harmonics. The stall cell travels at marginally higher frequencies of 70 Hz than half the rotor frequency of 67 Hz [7950/60 ∗ 2 = 67 Hz] at this operating speed. The stall cell is single and is fully developed.

4.3.1. 20% Axial Coverage. At 20% axial coverage with CT3-NP configuration, the stall cell travels at 70.5 Hz with reduced amplitude of the oscillations of 15.5 m/s. This amplitude is much lower than with the solid casing in place. Casing treatment provides damping and thus reduces the oscillations in the axial velocity at stall. The intensity of turbulence calculated at this location is 32.26% which is lower than with the solid casing and can be observed from Figures 14 and 17. At this coverage with addition of plenum chamber volume, the turbulence intensity reduces continuously. The lowest turbulence intensity of 15.57% was recorded for the CT3-FP configuration and can be seen from Figure 17. This shows that, at stall condition, the intensity of turbulence created by the casing treatment can be reduced by allowing the fluid to settle in the plenum chamber of the casing treatment. This increase in the plenum chamber acts as an additional damper, reducing the intensity further. With CT3-HP configuration, the stall cell moves at 71 Hz with an amplitude of 7.5 m/s and can be seen from Figure 15. At this coverage, when the compressor is coupled with the CT3-FP configuration, the stall cell travels with slightly higher speed of 73 Hz which corresponds to 55% of the rotor speed and can be seen from Figure 16. The amplitude in this case reduces further to 5 m/s. From this, it can be concluded that, in the presence of casing treatment with higher plenum volume, stall cell travels at relatively higher speed. For all the casing configurations at stall condition, the mean axial velocity recorded was around 64.5 m/s. However, the lowest RMS velocity of 9.98 m/s was

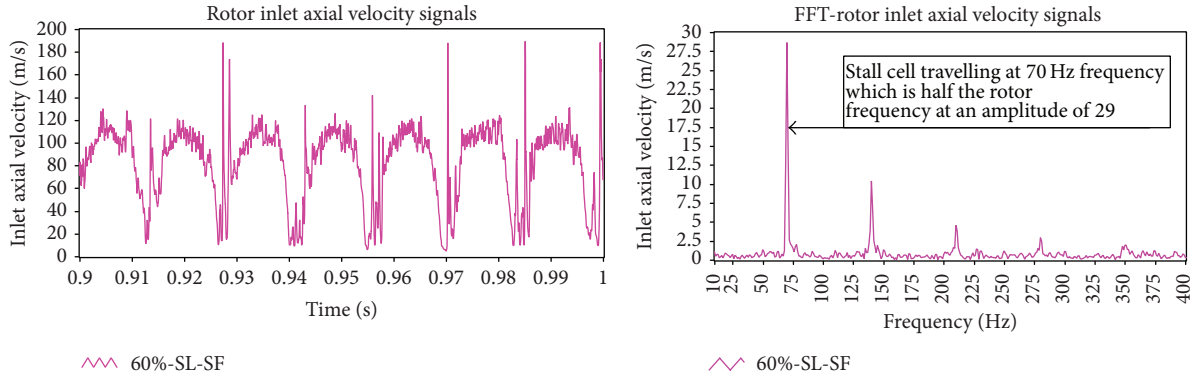

(a) Inlet axial velocity in the tip region ahead of the rotor leading edge

(b) FFT of inlet axial velocity showing the stall frequencies

Figure 13: Variation of inlet axial velocity for the solid casing at stall flow (SF) condition.

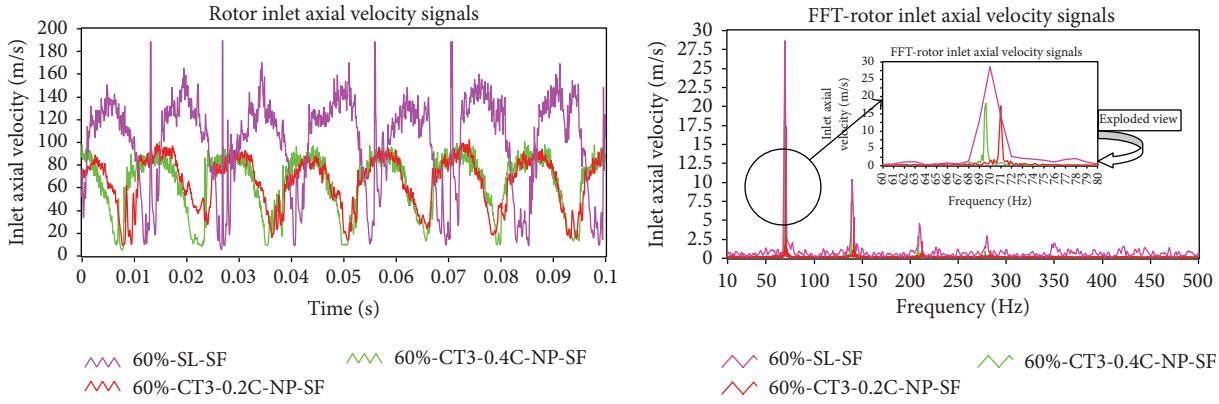

(a) Inlet axial velocity in the tip region ahead of the rotor leading edge for the solid casing and CT3-NP configuration

(b) FFT showing the stall frequency for the solid casing and CT3-NP configurations

Figure 14: Comparative variations of inlet axial velocity for the solid casing and CT3-NP configuration at 60% operating speed at stall flow (SF) condition for 20% and 40% axial coverage.

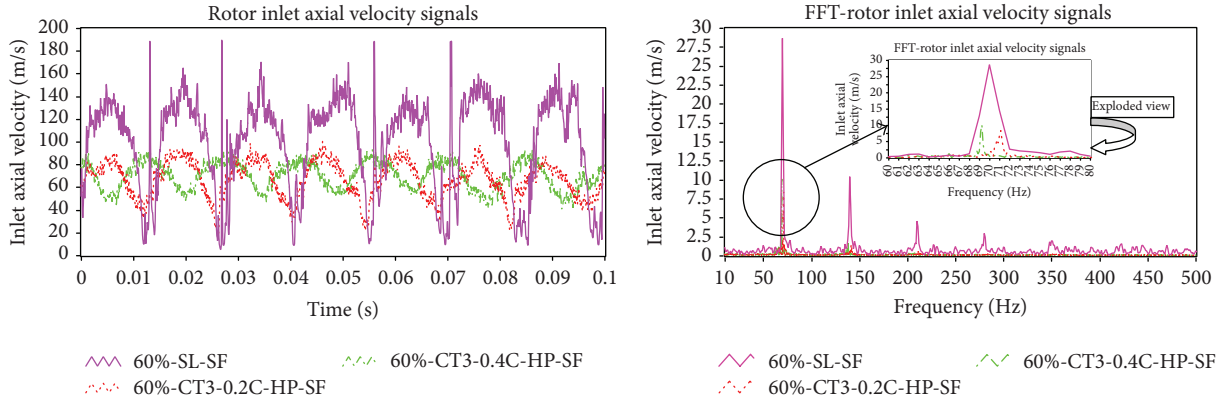

(a) Inlet axial velocity in the tip region ahead of the rotor leading edge for the solid casing and CT3-HP configuration

(b) FFT showing the stall frequency for the solid casing and CT3-HP configurations

Figure 15: Comparative variations of inlet axial velocity for the solid casing and CT3-HP configuration at 60% operating speed at stall flow (SF) condition for 20% and 40% axial coverage.

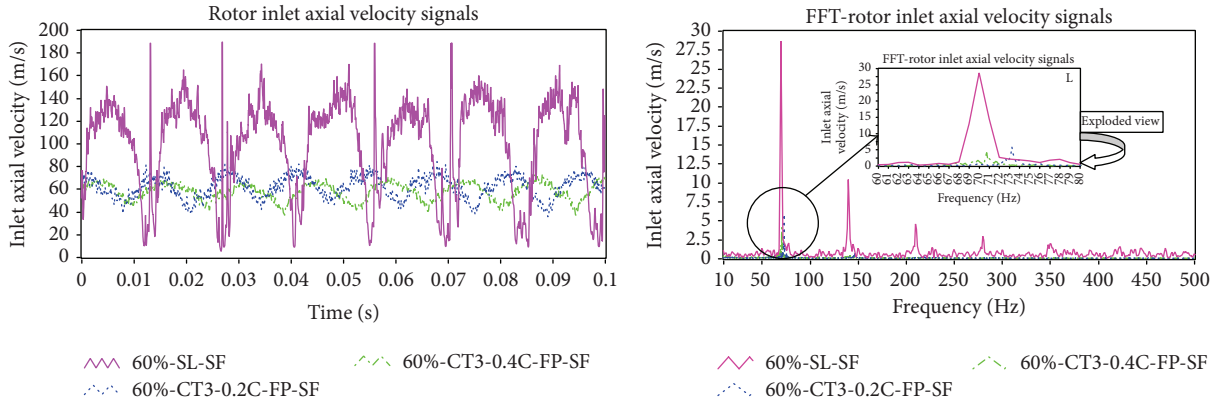

(a) Inlet axial velocity in the tip region ahead of the rotor leading edge for the solid casing and CT3-FP configuration

(b) FFT showing the stall frequency for the solid casing and CT3-FP configurations

FIGURE 16: Comparative variations of inlet axial velocity for the solid casing and CT3-FP configuration at 60% operating speed at stall flow (SF) condition for 20% and 40% axial coverage.

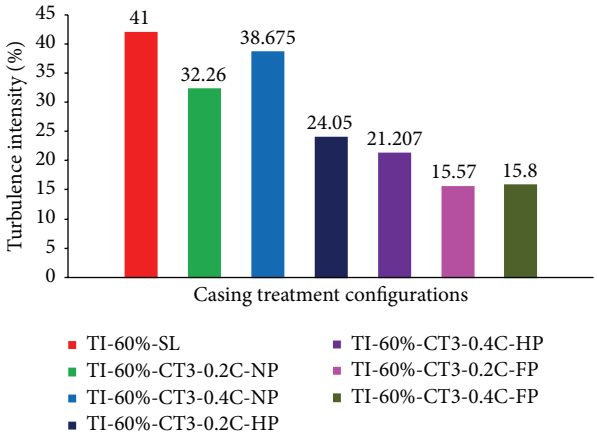

FIGURE 17: Comparative variations of turbulence intensity for the solid casing and casing treatment configuration at 60% operating speed at stall flow (SF) condition for 20% and 40% axial coverage.

recorded at CT3-FP, which reduces the turbulence intensity in this configuration.

4.3.2. 40% Axial Coverage. At 40% axial coverage with CT3-NP, the stall cell travels at 53% of the rotor speed, which corresponds to 69.5 Hz with slightly elevated amplitude of 17.5 compared to CT3-NP at 20% axial coverage. At this coverage, the mean velocity recorded was 65 m/s with turbulence intensity of 38.67% and can be observed from Figures 14 and 17. Higher turbulence intensity was recorded because of greater exposure of the casing treatment to the rotor. This further increases the interaction between the casing slots and air in the tip region. With CT3-HP configuration, the turbulence intensity reduces to 15.8% with the stall cell travelling at 69 Hz with amplitude of oscillations 10 m/s and can be observed from Figure 15. With increase in the plenum chamber volume to FP as shown in Figure 16, the amplitude of oscillations further comes down to 4.5 and stall cell travels at 71 Hz. For this configuration, the mean axial velocity of 61 m/s is recorded. The compressor stalls at relatively lower mass flow rates with this configuration at 40% axial coverage compared to other configurations.

From the above analysis, it is clear that the irrespective of the axial coverage, the amplitude of the oscillations, and turbulence level decrease with increase in the plenum chamber volume. All the casing treatment configurations reduce the intensity of stall as compared to the solid casing. With CT3-NP configuration, the nature of stall is similar to the solid casing, but with lower intensity. At both the axial coverages, with increase in the plenum chamber depth, the stall cell frequency remains more or less similar at the respective coverages.

5. Conclusions

Experimental studies on bend skewed casing treatment of 21% porosity have been carried out to study the impact of plenum chamber volume on the performance of a single stage transonic axial flow compressor. The following conclusions can be drawn based on this study.

(1) Peak stage efficiency of the compressor stage decreases significantly with increase in the operating speed. The peak stage efficiency decreases by 3.8% from 50% operating speeds to 80% of the design speed.

(2) Low porosity bend skewed casing treatment improves the stability margin of a single stage transonic axial flow compressor significantly.

(3) It is possible to enhance the performance of the compressor stage by incorporating the plenum chamber above the casing treatment. The stall margin increases with increase in the plenum chamber depth at both the axial coverages for 50% and 80% of the design speed.

(4) At 20% axial coverage and 80% design speed, all the three configurations of casing treatment show increase in the peak stage efficiency above the solid casing. This shows the positive effects of placing bend skewed casing treatment above the rotor in controlling the detrimental effects associated with the tip leakage flow.

(5) At 20% axial coverage and at all the operating speeds CT3-HP gives an optimum performancein terms of stall margin improvement and gain in the stage efficiency.

(6) At 70% operating speed and both the axial coverages CT3-NP configuration produces loss in the peak stage efficiency. At 20% coverage CT3-NP configuration improves the stall margin by 8.423% at the cost of 1.76% efficiency penalty. At 40% axial coverage the penalty in efficiency is 3.2% with 8.13% improvement in the stall margin.

(7) Maximum improvement in the stall margin of 29.16% is obtained at 50% operating speed with CT3-FP configurations at 40% axial coverage.

(8) Hot wire measurements reveal abrupt nature of stall in the presence of solid casing. Compressor stage stalls at higher mean axial velocity with very abrupt oscillations in the axial velocity. Axial velocity varies from 8 m/s to 185 m/s with very high turbulence intensity of 41% and amplitude of oscillations.

(9) Casing treatment provides damping and reduces the oscillations in the velocity associated with stall. At stall condition (SF) the mean axial velocity is much lesser than the solid casing. Lowest axial velocity of 61 m/s was recorded with CT3-FP configurations at 40% axial coverages.

(10) From the present experimental study it can be concluded that even with lower porosity bend skewed casing treatment and plenum chamber combination it is possible to achieve sufficient stall margin improvement and gain in the stage efficiency.

Nomenclature

Symbols

Π: Stage total pressure ratio
θ: Temperature ratio $\approx T_{\text{atm.}}/T_{\text{sealevel}}$, $T_{\text{sealevel}} \approx 288.15$ K
δ: Pressure ratio $\approx P_{\text{atm.}}/P_{\text{sealevel}}$, $P_{\text{sealevel}} \approx 1.01325$ bar
C: Axial chord at rotor tip (mm)
CT3: Casing treatment 3 with porosity of 21%
CT3-NP: Casing treatment with no plenum chamber configurations
CT3-HP: Casing treatment with half plenum chamber configurations
CT3-FP: Casing treatment with full plenum chamber configurations
CTA: Constant temperature anemometer
FF: Full flow condition (max mass flow condition)
EFF: Efficiency
FFT: Fast Fourier transform
FP: Full plenum chamber ≈ depth of plenum equals slot depth
HP: Half plenum chamber ≈ depth of plenum equals half the slot depth
$\dot{m}$: Mass flow rate (kg/s)
$\dot{m}_{\text{corrected}}$: Corrected mas flow rate (kg/s) = $\dot{m}\sqrt{\theta}/\delta$
N: Rotor rotation (RPM)
$N_{\text{corrected}}$: Corrected rotation (RPM) = $N/\sqrt{\theta}$
NP: No plenum chamber ≈ depth of plenum chamber zero
NSF: Near stall flow condition
P: Pressure (N/m^2)
R: Local blade radius (mm)
SF: Stall flow conditions
SMI: Stall margin improvements (%)
SL: Solid casing
TI: Turbulence intensity (%)
x: Width of the slots (mm)
y: Average width of the rib (mm)
0.2C: 20% rotor axial chord coverage
0.4C: 40% rotor axial chord coverage.

Suffix

SL: Solid casing
CT: Casing treatment
t: Tip radius
max: Maximum
atm: Atmospheric
s: Static condition
0: Total condition
1: Rotor inlet condition
2: Rotor exit condition
3: Stator exit condition.

Equation

$$\text{Porosity (\%)} = (x/(x+y)) \times 100.$$

Conflict of Interests

The authors declare that there is no conflict of interests regarding the publication of this paper.

Acknowledgments

The authors take this opportunity to thank Council of Scientific and Industrial Research, India, for providing financial support to carry out this research work. Acknowledgments are due to the Director, NAL, for giving permission to publish the experimental work. The authors gratefully acknowledge

the untiring efforts of Mr. Joseph Arulraj and Mr. G. S. Ravi, team members of axial flow compressor research (AFCR) facility. The authors would also like to thank the Propulsion Workshop staff for providing support during the fabrication and assembly. Support and encouragement received from Head Propulsion Division and Electrical Section, NWTC, Belur, are greatly recognized. Also special thanks are due to Mr. Veera Sheshakumar and Mr. Vijay Tijare for helping in rotor dynamics aspects. Relentless encouragement and motivation from Professor Q. H. Nagpurwala are accredited.

References

[1] E. M. Greitzer, J. P. Nikkanen, D. E. Haddad, R. S. Mazzawy, and H. D. Joslyn, "A fundamental criterion for the application of rotor casing treatment," *Transactions of the ASME, Journal of Fluids Engineering*, vol. 101, no. 2, pp. 237–243, 1979.

[2] C. C. Koch, "Experimental evaluation of outer casing blowing or bleeding of single stage axial flow compressor, Part VI," Final Report NASA CR-54592, 1970.

[3] W. Osborn and R. Moore, "Effect of outer casing treatment on overall performance of an axial flow compressor," NASA TMX 3477, 1977.

[4] D. Royce and W. Osborn, "Effect of tip clearance on overall performance of transonic fan stage with and without casing treatment," NASA TMX 3479, 1977.

[5] W. Osborn, "Effect of several porous casing treatments on stall limit and on overall performance of an Axial flow compressor rotor," NASA TND-6537, 1971.

[6] S. A. Guruprasad, "Experimental investigations on the influence of axial extension and location of outer casing treatment on the performance of an axial flow compressor," in *Proceedings of the 4th International Symposium on Experimental and Computational Aerothermodynamics of Internal Flows (AIF '99)*, Dresden, Germany, 1999.

[7] H. Takata and Y. Tsukuda, "Stall margin improvement by casing treatment—its mechanism and effectiveness," *Journal of Engineering for Gas Turbines and Power*, vol. 99, no. 1, pp. 121–133, 1977.

[8] H. Fujita and H. Takata, "A study on configurations of casing treatment for axial flow compressors," *Bulletin of the JSME*, vol. 27, no. 230, pp. 1675–1681, 1984.

[9] G. D. J. Smith and N. A. Cumptsy, "Flow phenomenon in compressor casing treatment," *Journal of Engineering for Gas Turbines and Power*, vol. 106, pp. 532–541, 1984.

[10] P. C. Adams and G. D. J. Smith, "The effect of axial slot casing treatment geometry on the stall margin improvement and efficiency of a low speed axial flow compressor," ISABE 87–7036, 1987.

[11] J. Zhu and W. Chu, "The effects of bend skewed groove casing treatment on performance and flow field near endwall of an axial compressor," in *Proceedings of the 43rd AIAA Aerospace Sciences Meeting and Exhibit*, pp. 14147–14154, Reno, NV, USA, January 2005.

[12] X. Lu, W. Chu, Y. Zhang, and J. Zhu, "Experimental and numerical investigation of a subsonic compressor with bend-skewed slot-casing treatment," *Proceedings of the Institution of Mechanical Engineers C: Journal of Mechanical Engineering Science*, vol. 220, no. 12, pp. 1785–1796, 2006.

[13] X. Lu, J. Zhu, C. Nie, and W. Huang, "The stability-limiting flow mechanisms in a subsonic axial-flow compressor and its passive control with casing treatment," in *Proceedings of the ASME Turbo Expo 2008: Power for Land, Sea and Air*, vol. 6, pp. 33–43, Berlin, Germany, June 2008.

[14] X. Lu, W. Chu, J. Zhu, and Y. Zhang, "Numerical investigations of the coupled flow through a subsonic compressor rotor and axial skewed slot," *Journal of Turbomachinery*, vol. 131, no. 1, 2009.

[15] M. Hembera, H. P. Kau, and E. Johann, "Simulation of casing treatments of a transonic compressor stage," *International Journal of Rotating Machinery*, vol. 2008, Article ID 657202, 10 pages, 2008.

[16] R. Emmrich, H. Hönen, and R. Niehuis, "Time resolved investigations of an axial compressor with casing treatment, part 1—experiment," in *Proceedings of the ASME Turbo Expo: Power for Land, Sea and Air*, GT2007-27581, Montreal, Canada, 2008.

[17] R. Emmrich, R. Kunte, H. Hönen, and R. Niehuis, "Time resolved investigations of an axial compressor with casing treatment part 2—simulation," in *Proceedings of the ASME Turbo Expo: Power for Land, Sea and Air*, pp. 199–208, Montreal, Canada, May 2007.

[18] R. Emmrich, H. Hönen, and R. Niehuis, "Time resolved experimental investigations of an axial compressor with casing treatment," *Journal of Turbomachinery*, vol. 131, no. 1, Article ID 011018, 9 pages, 2009.

[19] J. Streit, F. Heinichen, and P. Kau, "Axial-slot casing treatments improve the efficiency of axial flow compressors: aerodynamic effects of a rotor redesign," in *Proceedings of the ASME Turbo Expo. 2013 ,Turbine Technical Conference and Exposition*, GT2013- 94975, San Antonio, Tex, USA, 2013.

[20] M. Voges, C. Willert, R. Mönig, and H.-P. Schiffer, "The effect of a bend-slot casing treatment on the blade tip flow field of a transonic compressor rotor," in *Proceedings of the ASME Turbo Expo: Turbine Technical Conference and Exposition (GT '13)*, San Antonio, Tex, USA, June 2013.